Charge radii and electromagnetic moments of $^{214-218}$Bi: Exploring the "southern" border of the $Z > 82$ octupole-deformation region

A. Barzakh,[1,*] A. N. Andreyev,[2,3,†] Z. Yue,[2] L. Nies,[4] M. D. Seliverstov,[1] J. G. Cubiss,[2,‡] A. Algora,[5,6] B. Andel,[7] S. Antalic,[7] M. Al Monthery,[8] D. Atanasov,[9,4] J. Benito,[10] G. Benzoni,[11] T. Berry,[12] M. L. Bissell,[13] K. Blaum,[9] M. J. G. Borge,[14] K. Chrysalidis,[4,15] C. Clisu,[16] T. E. Cocolios,[17] C. Costache,[16] T. Day Goodacre,[18,4,19] G. J. Farooq-Smith,[17,§] D. V. Fedorov,[1] V. N. Fedosseev,[4] L. M. Fraile,[10] H. O. U. Fynbo,[20] V. Gadelshin,[15] L. P. Gaffney,[21,¶] R. F. Garcia Ruiz,[19,**] C. Granados,[4,17] P. T. Greenlees,[22] R. D. Harding,[2,4] L. J. Harkness-Brennan,[23] R. Heinke,[4,15,13] A. Herlert,[24] M. Huyse,[17] A. Illana,[25] J. Jolie,[26] D. S. Judson,[23] J. Karls,[4,27] J. Konki,[22] P. Larmonier,[4] I. Lazarus,[28] D. Leimbach,[4,27] R. Lică,[16] Z. Liu,[29,30] D. Lunney,[31] K. M. Lynch,[4,13] M. Madurga,[32] V. Manea,[4] N. Marginean,[16] R. Marginean,[16] B. A. Marsh,[4] C. Mihai,[16] P. Molkanov,[1] P. Mosat,[7] M. Mougeot,[4] J. R. Murias,[10] E. Nacher,[5] A. Negret,[16] D. Neidherr,[33] R. D. Page,[23] S. Pascu,[16] A. Perea,[14] V. Pucknell,[28] P. Rahkila,[22] C. Raison,[2] E. Rapisarda,[4] K. Rezynkina,[17] M. Rosenbush,[34,35] R. E. Rossel,[4] S. Rothe,[4] V. Sánchez-Tembleque,[10] K. Schomacker,[26] L. Schweikhard,[34] C. Seiffert,[4] S. Sels,[17,††] C. Sotty,[16] L. Stan,[16] M. Stryjczyk,[17,36] D. Studer,[15] J. Sundberg,[4,27] C. Sürder,[37] O. Tengblad,[14] P. Van Duppen,[17] V. Vedia,[10] M. Verlinde,[17] S. Viñals,[14] N. Warr,[26] A. Welker,[4,38] F. Wienholtz,[4,34,37] and R. N. Wolf[9,34,39]

[1] *Affiliated with an institute covered by a cooperation agreement with CERN at the time of the experiment*
[2] *School of Physics, Engineering and Technology, University of York, York YO10 5DD, United Kingdom*
[3] *Advanced Science Research Center, Japan Atomic Energy Agency, Tokai-mura, Ibaraki 319-1195, Japan*
[4] *CERN, 1211 Geneva 23, Switzerland*
[5] *Instituto de Física Corpuscular, CSIC - Universidad de Valencia, E-46980, Valencia, Spain*
[6] *HUN-REN Institute of Nuclear research (ATOMKI), P.O.Box 51, H-4001 Debrecen, Hungary*
[7] *Department of Nuclear Physics and Biophysics, Comenius University in Bratislava, 84248 Bratislava, Slovakia*
[8] *Physics Unit, College of Applied Sciences, University of Technology and Applied Sciences P.O. Box 74, AL Khuwair, Muscat 133, Oman*
[9] *Max-Planck-Institut für Kernphysik, Saupfercheckweg 1, 69117 Heidelberg, Germany*
[10] *Grupo de Física Nuclear, EMFTEL & IPARCOS, Facultad de Ciencias Físicas, Universidad Complutense de Madrid, 28040, Madrid, Spain*
[11] *Istituto Nazionale di Fisica Nucleare, Sezione di Milano, I-20133 Milano, Italy*
[12] *Department of Physics, University of Surrey, Guildford GU2 7XH, United Kingdom*
[13] *Department of Physics and Astronomy, The University of Manchester, Manchester M13 9PL, United Kingdom*
[14] *Instituto de Estructura de la Materia, CSIC, Serrano 113 bis, E-28006 Madrid, Spain*
[15] *Institut für Physik, Johannes Gutenberg-Universität, Mainz, D-55128 Mainz, Germany*
[16] *"Horia Hulubei" National Institute for R & D in Physics and Nuclear Engineering, RO-077125 Bucharest, Romania*
[17] *KU Leuven, Instituut voor Kern- en Stralingsfysica, B-3001 Leuven, Belgium*
[18] *TRIUMF, 4004 Wesbrook Mall, Vancouver BC V6T 2A3, Canada*
[19] *School of Physics and Astronomy, The University of Manchester, Manchester M13 9PL, United Kingdom*
[20] *Department of Physics and Astronomy, Aarhus University, DK-8000 Aarhus C, Denmark*
[21] *School of Engineering and Computing, University of the West of Scotland, Paisley, PA1 2BE, United Kingdom*
[22] *University of Jyväskylä, Department of Physics, P.O. Box 35, FI-40014, Jyväskylä, Finland*
[23] *Department of Physics, Oliver Lodge Laboratory, University of Liverpool, Liverpool L69 7ZE, United Kingdom*
[24] *FAIR GmbH, Planckstraße 1, 64291 Darmstadt, Germany*
[25] *Istituto Nazionale di Fisica Nucleare, Laboratori Nazionali di Legnaro, I-35020 Legnaro, Italy*
[26] *Institut für Kernphysik, Universität zu Köln, 50937 Köln, Germany*
[27] *Department of Physics, University of Gothenburg, SE-412 96 Gothenburg, Sweden*
[28] *STFC Daresbury, Daresbury, Warrington WA4 4AD, United Kingdom*
[29] *Institute of Modern Physics, Chinese Academy of Sciences, Lanzhou, 730000, China*
[30] *School of Nuclear Science and Technology, University of Chinese Academy of Sciences, Beijing 100049, China*
[31] *CSNSM-CNRS, Université de Paris Sud, 91400 Orsay, France*
[32] *Department of Physics and Astronomy, University of Tennessee, Knoxville, Tennessee 37996, USA*
[33] *GSI Helmholtzzentrum für Schwerionenforschung GmbH, Darmstadt 64291, Germany*
[34] *Institut für Physik, Universität Greifswald, 17487 Greifswald, Germany*
[35] *RIKEN Nishina Center for Accelerator-Based Science, Wako, Saitama 351-0198, Japan*
[36] *Institut Laue-Langevin, 71 Avenue des Martyrs, F-38042 Grenoble, France*
[37] *Institut für Kernphysik, Technische Universität Darmstadt, 64289 Darmstadt, Germany*
[38] *Institut für Kern- und Teilchenphysik, Technische Universität Dresden, Dresden 01069, Germany*

[39]36 ARC Centre of Excellence for Engineered Quantum Systems,
School of Physics, The University of Sydney, NSW 2006, Australia
(Dated: Monday 1st September, 2025)

The changes in the mean-squared charge radii relative to ^{209}Bi$_{126}$ ($\delta\langle r^2\rangle^{N,126}$), the magnetic dipole and electric quadrupole moments in $^{214-218}$Bi have been measured using the in-source resonance-ionization spectroscopy technique at ISOLDE (CERN). Magnetic moments of odd-odd bismuth nuclei have been analyzed by the additivity relation. Previous tentative spin-parity and configuration assignments based on the β-decay feeding patterns have been supported. A normal odd-even staggering in charge radii of bismuth isotopes with $N > 126$ has been observed. The new data for the $\delta\langle r^2\rangle$ of bismuth isotopes allow a study of the isotonic dependencies in the charge radii, revealing jumps in $\delta\langle r^2\rangle^{132,126}$ and $\delta\langle r^2\rangle^{134,126}$ at $Z = 84$. This pattern could be explained by a sudden onset of octupole deformation at $N = 132$ and 134 when going from polonium ($Z = 84$) to astatine ($Z = 85$).

I. INTRODUCTION

For nuclei with $130 \leqslant N \leqslant 140$ and $85 \leqslant Z \leqslant 92$, the possible presence of octupole deformation (reflection asymmetry in the intrinsic frame) was predicted long ago and its extensive experimental proofs exist by now (see e.g. Refs. [1–7] and references therein). Interest in the reflection asymmetry phenomena for trans-lead nuclei is strongly fueled by the prediction that nuclear octupole deformation significantly enhances P-odd and T-odd nuclear electromagnetic moments, making reflection asymmetric nuclei the first choice candidates in the search for permanent atomic electric-dipole moments and physics beyond the Standard Model [8, 9].

There are several phenomena which are taken as evidence for octupole collectivity, namely, interleaved positive- and negative-parity rotational bands in even-even nuclei, parity doublets in odd-mass nuclei, enhanced $E1$ and $E3$ transition strengths, peculiarities in the magnetic-moment and decoupling-parameter behavior, etc. [1, 2].

Evidence for octupole deformations can also be found in the behavior of the nuclear radii. For example, charge radii, calculated in the framework of the finite-range droplet model and the energy density functional approach are in better agreement with experiment when reflection asymmetry is included [10, 11].

Another sign of octupole effects in this region is a so-called inverse odd-even staggering (inverse OES) in the charge radii. As a rule, nuclear charge radii of odd-N isotopes are smaller than the average of their even-N neighbors (normal OES) [12, 13]. Inverse OES, when the odd-N isotope has a larger radius than the average of its even-N neighbors, is considered as the possible evidence of octupole collectivity [14]. The correlation between octupole deformation and inverse OES was qualitatively described by Otten [14, 15] and corroborated by the calculations of Leander and Sheline [16].

Near $N = 133$ inverse OES was found for $_{85}$At [17], $_{86}$Rn [15, 18], $_{87}$Fr [19] and $_{88}$Ra [14, 20]. At the same time, the charge radii of $_{84}$Po isotopes display normal OES near $N = 133$ [21]. This suggests that polonium isotopes represent the "southern" boundary of the inverse OES (i.e. presumably octupole) region at least for $N = 133$. In the present work, we have measured the changes in the mean squared charge radii of $^{214-218}_{83}$Bi$_{131-135}$ relative to ^{209}Bi$_{126}$ ($\delta\langle r^2\rangle_{A,209}$) to study the OES in radii near $N = 133$ for bismuth isotopes. Our results complete the systematics of nuclear charge radii with $126 \leqslant N \leqslant 134$ and $82 \leqslant Z \leqslant 88$ and allow us to analyze the isotonic dependencies of $\delta\langle r^2\rangle$ and possible influence of octupole collectivity on their trends.

II. EXPERIMENTAL DETAILS

The experiments were performed at the ISOLDE facility (CERN) [22]. Bismuth nuclei were produced in spallation reactions induced by the 1.4-GeV proton beam from the CERN PS Booster impinging on a thick UC$_x$ target (50 g cm^{-2} of ^{238}U). The spallation products effused out of the high-temperature target ($T \approx 2500$ K) as neutral atoms into the cavity of the Resonance Ionization Laser Ion Source, RILIS [23]. The bismuth atoms were resonantly ionized when the laser beams were wavelength-tuned to a three-step ionization scheme [24, 25]. The produced photoions were extracted and accelerated by a 30-kV potential and mass separated by ISOLDE's General Purpose Separator or High Resolution Separator.

The hyperfine structure (hfs) and isotope shift (IS) measurements were performed for the first-step transition $6p^3\ ^4S^o_{3/2} \rightarrow 6p^2(^3P_0)7s\ ^2[0]_{1/2}$ ($\lambda_1 = 306.9$ nm) by scanning the frequency of the narrowband Titanium Sapphire laser with a typical full width half-maximum bandwidth of ≈ 600 MHz [26].

* barzakh_ae@pnpi.nrcki.ru
† andrei.andreyev@york.ac.uk
‡ Present address: School of Physics and Astronomy, University of Edinburgh, Edinburgh, EH9 3FD, United Kingdom
§ Present address: Department of Oncology Physics, Edinburgh Cancer Centre, Western General Hospital, Crewe Road South, Edinburgh, EH4 2XU, United Kingdom
¶ Present address: Oliver Lodge Laboratory, University of Liverpool, Liverpool L69 7ZE, United Kingdom
** Present address: Department of Physics, Massachusetts Institute of Technology, Cambridge, USA
†† Present address: CERN, 1211 Geneva 23, Switzerland

Data were collected during three separate experimental runs which differ by the method of photoion-current monitoring. During the first experiment (2016), the photoion current of ^{218}Bi was monitored using the Windmill decay station (WM) [27] by detecting the characteristic α decays of the β-decay daughter ^{218}Po, while for ^{215,217}Bi^{g} and the ^{216}Bi^{g+m} mixture, the monitoring was accomplished by ion counting with the ISOLTRAP Multi-Reflection Time-of-Flight Mass-Separator (MR-ToF MS) [28, 29]. In the course of the second (2017) and third (2018) experimental runs, the ISOLDE Decay Station (IDS) [30] was used to detect characteristic α and γ decays of $^{214-217}$Bi^{g} and ^{214,216}Bi^{m}. Partial results from these studies have been presented in Refs. [31–34].

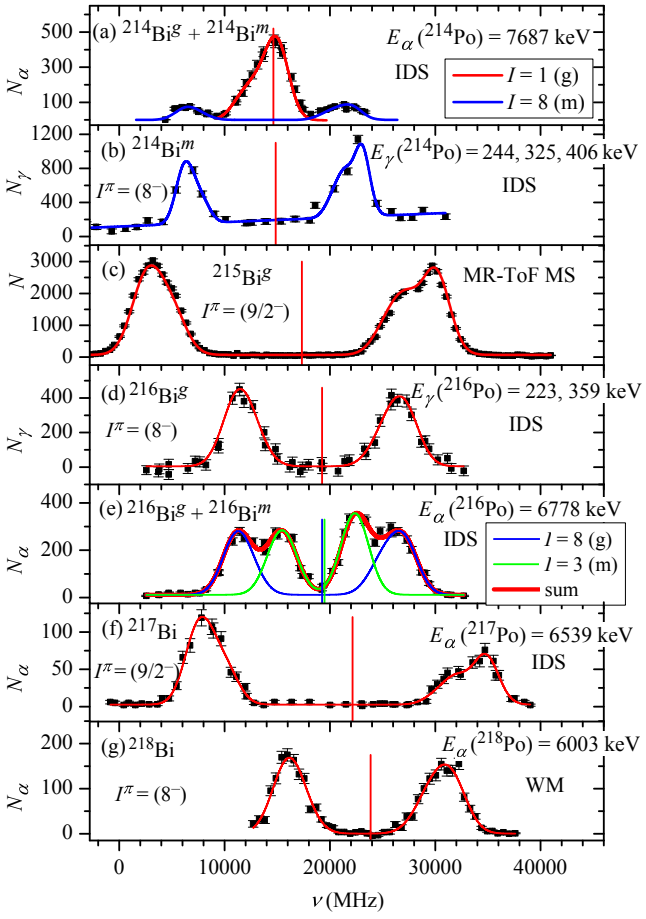

FIG. 1. Examples of the hfs spectra for bismuth isotopes. The preferable nuclear spins (see discussion in Sec. V), measurement device and α- and γ-decay energies when using IDS or WM, are shown. The solid lines depict the Voigt-profile fit to the data. The vertical lines mark the centroids of the corresponding hfs. The zero point on the frequency scale corresponds to a wave number of 32588.16 cm^{-1}.

III. RESULTS

Several hfs spectra were obtained for each of the investigated nuclides during each experimental campaign. Figure 1 provides typical examples. The upward slope in ^{214}Bi^{g} hfs [see Fig. 1 (b)] is connected with the increase of the background due to accumulation of the long-lived isotopes in the specific experimental conditions (for example, ^{210}Rn from the decay of ^{214}Ra).

In ^{216}Bi, two long-lived, β-decaying states are known: a low-spin, $I^\pi = (3^-)$[1], and a high-spin, $I^\pi = (8^-)$ [40]. Due to the large uncertainty of the low-spin isomer excitation energy of 24(19) keV [41], the order of the states in ^{216}Bi is not firmly established, but for consistency with the literature [33, 39–41], the high-spin state will be referred to as ^{216}Bi^{g}.

For ^{214}Bi, as well as the well-known ground state with $I^\pi = 1^-$ [42, 43], the high-spin, long-lived β-decaying isomer with $I^\pi = (8^-)$ was found [31].

The presence of long-lived β-decaying isomers in ^{214,216}Bi complicates the analysis of the corresponding hfs. Photoion-current monitoring by the α decay of the daughter ^{214,216}Po gives the mixed hfs, since the corresponding polonium nuclei are produced in the β decay of both isomeric and ground states, see Fig. 1 (a, e).

However, it is possible to obtain pure hfs spectra of the high-spin states in ^{214,216}Bi using the difference in the β decay schemes for the low- and high-spin states. In the case of the high-spin ^{216}Bi^{g}, see Fig. 1 (d), γ lines of 223 and 359 keV (the $8^+ \to 6^+$ and $6^+ \to 4^+$ transitions in daughter ^{216}Po) were monitored at IDS as the 8^+ and 6^+ ^{216}Po states are not populated in the β decay of the low-spin ^{216}Bi^{m} [33] and therefore only ^{216}Bi^{g} hfs is presented in the experimental spectrum. Similarly, a pure ^{214}Bi^{m} [$I^\pi = (8^-)$] hfs was extracted by monitoring γ lines of 244, 325, and 406 keV corresponding to $8^+ \to 6^+$, $6^+ \to 4^+$, and $4^+ \to 2^+$ transitions in daughter ^{214}Po, see Fig. 1 (b).

The positions of the hyperfine components in the hfs spectra are determined by the standard relation [15] with five parameters: nuclear spin (I), the IS relative to stable ^{209}Bi ($\delta\nu_{A,209}$), magnetic hfs constants (a_1 and a_2) for the first ($6p^3\ ^4S^o_{3/2}$) and second ($6p^2(^3P_0)7s\ ^2[0]_{1/2}$) levels of the ionization scheme, and the electric quadrupole hfs constant b_1 for the first level. Note, that the electric quadrupole hfs constant for the second level $b_2 \equiv 0$ since the second level has total electronic angular momentum $J = 1/2$.

Due to the limited resolution of the RILIS method we cannot determine nuclear spin from the hfs spectra alone. Therefore, we were forced to use available information on the spin values obtained by nuclear spectroscopy. For

[1] Here and below we used preferable spin values in accordance with Refs. [31, 33, 35–39]. In the present work these assignments were supported (see Sec. V). Other spin options are considered in Appendix A.

TABLE I. Preferred spin-parity assignments (I^π), IS ($\delta\nu_{A,209}$), hfs constants (a_2, b_1), changes in mean-squared charge radius ($\delta\langle r^2\rangle_{A,209}$), magnetic ($\mu$) and quadrupole ($Q_s$) moments for investigated Bi nuclei. In the seventh column the results of the additivity-relation calculation for odd-odd nuclides are shown ($\mu_{\rm add}$), see Sec. V. The statistical and systematic uncertainties of $\delta\langle r^2\rangle_{A,209}$ and μ are shown in round and curly brackets, respectively. The latter values originate from the uncertainty of the F and M factors for $\delta\langle r^2\rangle_{A,209}$ and from the uncertainty of the hyperfine anomaly for μ.

A	I^π	$\delta\nu_{A,209}$ (MHz)	$\delta\langle r^2\rangle_{A,209}$(fm^2)	a_2 (MHz)	$\mu(\mu_N)$	$\mu_{\rm add}(\mu_N)$	b_1(MHz)	Q_s(b)
214g	1^-	12750(140)	0.532(6){23}	1438(130)	0.265(24){3}	0.28	0[a]	0
214m	(8^-)	12880(300)	0.538(13){23}	1520(70)	2.25(10){2}	2.26	−230(500)	−0.31(69)
215g	$(9/2^-)$	15550(100)	0.649(4){28}	4423(40)[b]	3.675(33){18}[b]		−397(150)[b]	−0.55(21)[b]
216g	(8^-)	17520(130)	0.731(5){31}	1523(25)	2.249(37){22}	2.27	−120(100)	−0.17(14)
216m	(3^-)	17670(160)	0.738(7){31}	1774(40)	0.983(22){10}	0.86	630(200)	0.87(28)
217	$(9/2^-)$	20280(120)	0.846(5){36}	4465(50)[b]	3.710(42){37}[b]		−520(150)[b]	−0.72(21)[b]
218	(8^-)	22350(160)	0.933(7){40}	1501(14)	2.218(21){22}	2.30	810(200)	1.12(28)

[a] Fixed.
[b] Reference [34].

^{215,217}Bi^g, $I = 9/2$ was fixed in accordance with systematics and shell-model calculations [35–37]. The indeterminacy in spin assignment exists for ^{214,216}Bi. The $I = 8$ assignment is regarded as preferable for ^{214}Bi^m and ^{216}Bi^g but the possibility of $I = (7, 9)$ cannot be strictly excluded [31, 33]. For ^{216}Bi^m, while the most probable assignment is $I = 3$, $I = 2$ or 4 cannot be definitely ruled out [33]. In the case of ^{218}Bi, only a range of possible spins $I = 6, 7, 8$ can be established based on the β-decay feeding pattern [38, 39]. However, as will be shown in Sec. V by the magnetic moment analysis, the preferable assignment for ^{218}Bi is $I = 8$. Note that the same spin for the ^{218}Bi ground state was predicted by shell-model calculations [38].

Experimental data were fitted with Voigt profiles (more details are in Ref. [25]). In the fit, the ratio $\rho = a_2/a_1$ was fixed according to its value for ^{209}Bi: $\rho(^{209}\text{Bi}) = -11.013(4)$ [44, 45]. The fitting results (a_2, b_1 hfs constants values and values of IS) from different runs agree with each other within the limits of uncertainties and the final values presented in Table I are the corresponding weighted means. Only the values obtained with the preferred spins are shown, while the other (less probable) spin options are considered in Appendix A for completeness.

From the hfs constants, the nuclear magnetic dipole moments μ and electric quadrupole moments Q_s were deduced relative to the values for ^{209}Bi from Refs. [32, 45]. It was found (see Ref. [45]) that the hyperfine anomaly (HFA) is not negligible for bismuth isotopes when the $6p^2(^3P_0)7s\ ^2[0]_{1/2}$ atomic state is used for μ determination. High-resolution hfs measurements for lighter bismuth isotopes demonstrate that the HFA for states with spin 9/2 is less than 0.5% whereas for other spins it does not exceed 1% [46]. The corresponding uncertainties were taken into account for the μ values in Table I. The electronic factors F and M needed to extract $\delta\langle r^2\rangle$ from the measured IS, see Eqs. (8 and 9) in Ref. [47], were determined in Ref. [32] by advanced atomic calculations: $F = 23.8(10)$GHz fm^{-2} and $M = -750(100)$ GHz u. The values of μ, Q_s, and $\delta\langle r^2\rangle$ are presented in Table I. It is impossible to extract Q_s value from the unresolved hfs of ^{214}Bi^g, see Fig. 1 (a). Similarity of the structure of $I^\pi = (1^-)$ ground states of ^{212}Bi and ^{214}Bi points to the similarity of their Q_s. It was found in Ref. [48] that $b_1(^{212}\text{Bi})$=80(225)MHz and $Q_s(^{212}\text{Bi})$=0.11(31). Correspondingly, in fitting, hfs constant $b_1(^{214}\text{Bi}^g)$ was fixed, $b_1(^{214}\text{Bi}^g)$=0 MHz. The change of the fitting parameters due to variation of this constant in the limits of ±400 MHz was included in the uncertainties.

IV. CHARGE RADII

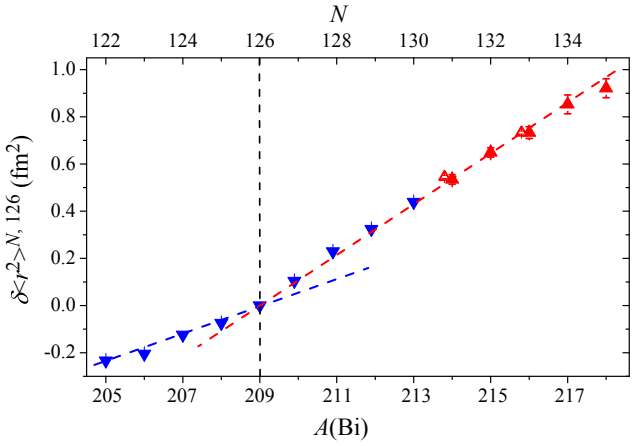

FIG. 2. Changes in the nuclear mean-squared charge radii for bismuth isotopes with $N > 121$ (upward triangles: present work; downward triangles: Refs. [48, 49]). Full and hollow symbols label the ground states and isomers, respectively. The symbols are connected by dashed lines to guide the eyes.

In Fig. 2, the deduced $\delta\langle r^2\rangle$ values with systematic and statistical uncertainties added in quadrature, are plotted

versus A. In the most cases this total $\delta\langle r^2\rangle$ uncertainty is less than the data-point size. Linear trends with different slopes are seen above and below $N = 126$ confirming the kink at $N = 126$. Our new data demonstrate that the linear trend is preserved for $131 \leq N \leq 135$. The isomers and ground states in ^{214,216}Bi presumably belong to the same $\pi 1h_{9/2} \otimes \nu 2g_{9/2}$ multiplet (see [31, 33]). Due to this, the deduced isomer shifts for these isomers are negligible within the limits of uncertainties.

A. Odd-even staggering in charge radii

In order to quantitatively compare the magnitude of the OES in different isotopic chains, the staggering indicator (γ_N; N is odd) is used [50]:

$$\gamma_N = \frac{2\delta\langle r^2\rangle^{N-1,N}}{\delta\langle r^2\rangle^{N-1,N+1}}. \quad (1)$$

This indicator is independent of the uncertainties in the atomic F factor (usually $5 - 10\%$ in the lead region). Normal OES corresponds to $\gamma_N < 1$, whereas $\gamma_N > 1$ points to inverse OES.

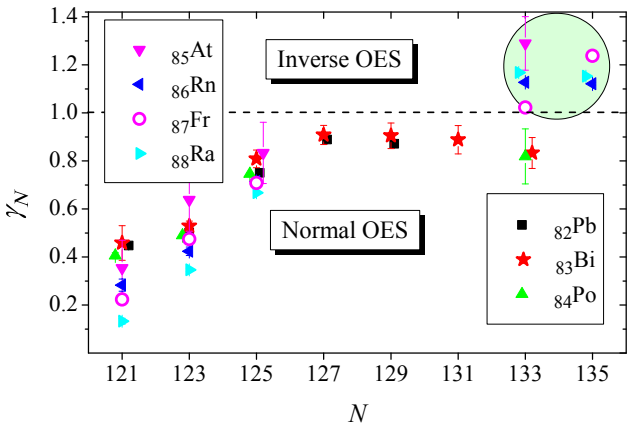

FIG. 3. Staggering indicator γ_N for Pb-Ra isotopes ($Z = 82 - 88$) at $N = 121 - 135$. Data are from Refs. [15, 17–19, 21, 48, 49, 51–57] and the present work. The green-shaded circle outlines the region of the inverse OES at $N < 136$.

The staggering indicator for bismuth isotopes near $N = 126$ is shown in Fig. 3 together with corresponding literature data for isotopic chains with $Z = 82 - 88$. As seen in Table III, the difference between $\delta\nu_{A,209}$ obtained with different spin assignments, is negligibly small in comparison with the IS uncertainties. Correspondingly, γ_N is independent on the plausible spin assignments. Similarly, another ordering of the ground and isomeric states in ^{216}Bi would not change γ_{133}(Bi) due to the negligible isomeric shift.

Inverse OES is observed for $_{88}$Ra, $_{87}$Fr, $_{86}$Rn, and $_{85}$At isotopes with $N = 133, 135$ (see data in the green-shaded circle in Fig. 3), whereas normal OES at $N = 133$ is restored for $_{84}$Po isotopes. According to our results, the bismuth isotopes keep the normal OES for $N = 133$ as well. Thus, our data confirm the assumption that $Z = 84$ is the "southern" boundary for the inverse-OES region at $N = 133$ [21]. A clear jump of the staggering indicator is seen when going from $Z = 83, 84$ (bismuth, polonium; $\gamma_{133} \approx 0.8$) to $Z = 85, 86$ (astatine, radon; $\gamma_{133} \approx 1.2$). Presumably, this jump may indicate an abrupt onset of octupole deformation for $Z \geqslant 85$ at $N = 133$.

B. Isotonic dependence of $\delta\langle r^2\rangle$ at $N \geqslant 126$

Our new data complete the systematics of nuclear charge radii at $82 \leqslant Z \leqslant 88$ and allow us to analyze the isotonic dependencies of $\delta\langle r^2\rangle$ and search for the possible influence of octupole collectivity on their trends.

TABLE II. Wavelength of atomic transitions used for IS measurements (λ), electronic factor (F) for these transitions, and total relative uncertainty of $\delta\langle r^2\rangle$.

Z	λ(nm)	F(GHz fm^{-2})	Uncertainty of $\delta\langle r^2\rangle$ (%)	Ref.
82	283	20.3	9	[51, 58]
83	307	23.8	5	[32]
84	843	-12.8	5	[52, 53]
85	795	-11.6	5	[54]
86	745	-19.2[a]	10	
87	718	-20.8	3	[55, 56]
88	468	-39.8	5	[57]

[a] Corrected semiempirical F factor from Refs. [15, 18], see Appendix B for details.

The estimation of systematic uncertainties (see Table I) is of key significance, when the $\delta\langle r^2\rangle$ values for different isotopic chains are compared. These uncertainties stem primarily from the uncertainty of the electronic F factor. The F values and total relative uncertainties used in the calculations of the isotonic $\delta\langle r^2\rangle$ dependencies are summarized in Table II, see Appendix B for details.

In Fig. 4, $\delta\langle r^2\rangle$ values for bismuth isotopes near $N = 126$ are compared with the data for isotonic nuclei with $Z = 82-88$. Total uncertainties in the most cases are less than the data-point size. The $\delta\langle r^2\rangle$ values for all of these isotopic chains are nearly indistinguishable at $N < 126$, whereas at $N > 126$ two groups are clearly seen, one including At-Ra isotopes and other with Pb-Po nuclei. Namely, the gradient in $\delta\langle r^2\rangle$ is nearly independent of Z in each group and it is markedly larger for At, Fr, and Ra chains ($Z = 85, 87, 88$) than for Pb, Bi, and Po isotopes ($Z = 82, 83, 84$).

In Fig. 5, the isotonic dependencies of the $\delta\langle r^2\rangle^{132,126}$, $\delta\langle r^2\rangle^{134,126}$ and $\delta\langle r^2\rangle^{126,122}$ values are shown, in order to better visualize the observed effect. We preferred to analyze the isotonic dependencies of $\delta\langle r^2\rangle$ rather than absolute $\langle r^2\rangle$ values to avoid the increase of uncertainties from usually poorly known (or even unknown) reference

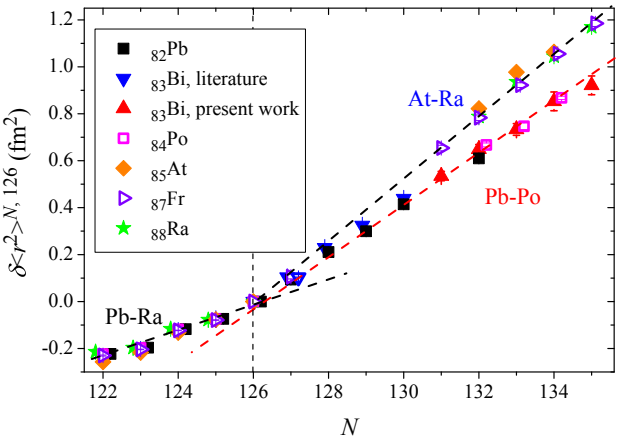

FIG. 4. Changes in the mean-squared charge radii for isotopic chains near $Z = 82$ and $N = 126$: $_{82}$Pb, full squares, Ref. [51]; $_{83}$Bi, downward triangles, Refs. [48, 49] and present work; $_{84}$Po, hollow squares, Refs. [21, 52] (recalculated with atomic factors from Ref. [53]); $_{85}$At, diamonds, Refs. [17, 54]; $_{87}$Fr, rightward triangles, Refs. [55, 56]; $_{88}$Ra, stars, Ref. [57].

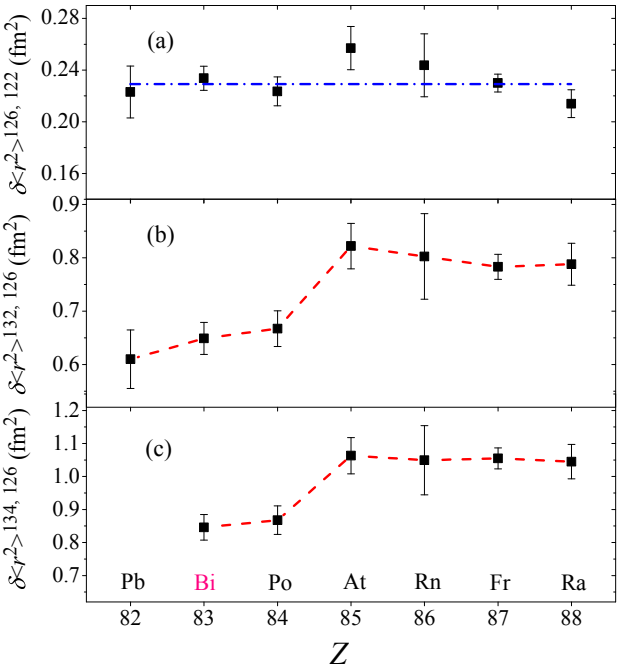

FIG. 5. Isotonic dependence of (a) $\delta\langle r^2\rangle^{126,122}$, (b) $\delta\langle r^2\rangle^{132,126}$, and (c) $\delta\langle r^2\rangle^{134,126}$. The radon ($Z = 86$) data from Refs. [15, 18] were recalculated with the atomic factor scaled in accordance with its typical overestimation by the semiempirical method used in Ref. [15], see details in Appendix B. Other experimental data are from the same sources as in Fig. 4. In panel (a) the dot-dashed line represents the weighted mean of the $\delta\langle r^2\rangle^{126,122}$ values. In panels (b) and (c), the dashed lines connect the data points to guide the eyes.

absolute $\langle r^2\rangle$ values [2].

The $\delta\langle r^2\rangle^{126,122}$ values for $Z = 82-88$ coincide within the limits of uncertainties, see Fig. 5 (a). In contrast, $\delta\langle r^2\rangle^{132,126}$ and $\delta\langle r^2\rangle^{134,126}$ demonstrate marked jumps when going from $Z = 84$ (polonium) to $Z = 85$ (astatine). Note, that these jumps occur at the same Z values as in the case of the OES at $N = 133$ (see Fig. 3). It is natural to suppose that such a jump in the isotonic dependencies of $\delta\langle r^2\rangle$ is due to an abrupt onset of octupole deformation.

The possible gain in the $\delta\langle r^2\rangle$ value ($\delta\langle r^2\rangle_{\rm oct}$) due to an increase in the octupole-deformation parameter, β_3, can be estimated by the formula [14, 15, 62]:

$$\delta\langle r^2\rangle_{\rm oct}^{N_1,N_2} = \frac{5}{4\pi}\langle r_0^2\rangle^{\overline{N}}\delta\langle\beta_3^2\rangle^{N_1,N_2}. \qquad (2)$$

where $\overline{N} = (N_1 + N_2)/2$ and $\langle r_0^2\rangle^N$ is a mean-squared charge radius of the isotope with N neutrons [12]. This gain should be compared with the experimental value of the observed jumps (see Fig. 5) $\delta\langle r^2\rangle^{132}_{\rm jump} \equiv \delta\langle r^2\rangle^{132,126}({\rm At}) - \delta\langle r^2\rangle^{132,126}({\rm Po}) = 0.16(5)$ fm^2, $\delta\langle r^2\rangle^{134}_{\rm jump} \equiv \delta\langle r^2\rangle^{134,126}({\rm At}) - \delta\langle r^2\rangle^{134,126}({\rm Po}) = 0.20(7)$ fm^2.

With β_3(Po)=0 and assuming that the whole effect originates from octupole degree of freedom, an agreement with experiment requires $\beta_3({\rm At}_{132})$=0.112(18) and $\beta_3({\rm At}_{134})$=0.125(25) in Eq. (2). However, it is possible that some fraction of the observed jump could be due to a quadrupole deformation β_2. One can estimate this contribution using, for example, the β_2 values from the macroscopic-microscopic calculations in Ref. [63]: $\beta_2({\rm Po}_{132})$=0.02, $\beta_2({\rm Po}_{134})$=0.039, $\beta_2({\rm At}_{132})$=0.039, $\beta_2({\rm At}_{134})$=0.103. Then, the agreement with experiment will be obtained with $\beta_3({\rm At}_{132})$=0.107(18) and $\beta_3({\rm At}_{134})$=0.083(15).

These values are compatible with the β_3 value ($\beta_3 = 0.10$) ascribed to the odd-A Rn, Fr, Ra, Ac, Th isotopes with $131 \leqslant N \leqslant 140$ in Ref. [64]. In the framework of the macroscopic-microscopic calculations [3, 63] similar values ($|\beta_3| = 0.12 - 0.13$) were predicted in the region $131 \leqslant N \leqslant 136$, $85 \leqslant Z \leqslant 88$. Recent calculations with five Skyrme energy-density functionals also predict $\beta_3 \approx 0.10$ for radium and radon isotopes with $N = 132, 134$ (see Fig. 6 in Ref. [7]).

V. MAGNETIC MOMENTS OF ODD-ODD ^{214,216,218}BI

Comparison of the experimental magnetic moments of the odd-odd nuclei with the estimates from the additivity

[2] For the previous attempts to analyze the $\langle r^2\rangle$ isotonic dependencies see Refs. [12, 59–61]. Note, that the absence of the experimental data on the absolute $\langle r^2\rangle$ values for Po, At, Rn, Fr, Ra hinders the extension of the isotonic-dependencies analysis in the framework of these approaches in this region.

relation (see Ref. [65] and references therein), $\mu_{\rm add}$, facilitates understanding nucleon orbital occupations and indicates the most probable spin of the nuclei in question.

Magnetic moments for odd-A ^{215,217}Bi were measured and discussed in Ref. [34]. It was shown that the further one moves from the magic $N = 126$, the larger the admixtures of other configurations to the leading one ($\pi 1h_{9/2}$) become [34].

The most probable configuration for odd-odd bismuth isotopes with $126 < N < 135$ is $\pi 1h_{9/2} \otimes \nu 2g_{9/2}$ (see Refs. [31, 33] and references therein). We compared our experimental data with the results of the additivity-relation calculations for different members of this multiplet. The above mentioned configuration mixing is effectively taken into account when in the framework of the additivity-relation calculations, individual empirical μ values for the $\pi 1h_{9/2}$ and $\nu 2g_{9/2}$ orbitals were taken from the available magnetic moments of the closest odd-A polonium and bismuth isotopes (see Refs. [34, 48, 66, 67]).

As seen from Table I and Table III (Appendix A), the $I^\pi = (8^-)$ assignment gives the best agreement between $\mu_{\rm add}$ and $\mu_{\rm expt}$ for ^{214}Bi^m, ^{216}Bi^g and ^{218}Bi. Thus, our magnetic-moment data support the $I^\pi = (8^-)$ assignments for ^{214}Bi^m and ^{216}Bi^g made in Refs. [31, 33]. The $\mu_{\rm add}$ value assuming $I^\pi = (3^-)$ gives a better description of the experimental μ than with $I^\pi = 2^-$ or 4^-. Note, that the additivity-relation calculation fails to reproduce μ for isotonic ^{218}At with a 40% discrepancy relative to the experimental value [17]. This difference was attributed to the possible influence of the octupole collectivity [17]. In contrast, a satisfactory description of $\mu(^{216}\text{Bi}^m)$ by the additivity relation supports the inference of the absence of noticeable octupolarity in ^{216}Bi.

VI. SUMMARY

To summarize, IS and hfs were studied for neutron-rich bismuth nuclei $^{214-218}$Bi^g and ^{214,216}Bi^m using the in-source resonance-ionization spectroscopy technique. Magnetic dipole and electric quadrupole moments were derived from the analysis of hfs. The I^π assignments for the odd-odd nuclides, $I^\pi(^{214}\text{Bi}^m) = (8^-)$, $I^\pi(^{216}\text{Bi}^g) = (8^-)$, and $I^\pi(^{216}\text{Bi}^m) = (3^-)$, proposed by β-decay studies [31, 33], are supported by the comparison of the measured magnetic moments with the results of the additivity-relation calculations.

Jumps in the isotonic dependencies of $\delta\langle r^2\rangle^{126,132}$ and $\delta\langle r^2\rangle^{126,134}$ when going from $Z = 84$ to $Z = 85$ were observed. This pattern, as well as the behavior of the OES, could be explained by the assumption of a sudden onset of octupole deformation at $N = 132 - 134$ when going from $Z = 84$ to $Z = 85$.

Additional measurements by other techniques, especially those which are more directly able to measure octupole deformation, such as Coulomb excitation (COULEX), to help understand the nature of reflection asymmetry in this region, would be important.

ACKNOWLEDGMENTS

We thank the ISOLDE Collaboration for providing excellent beams. This work was supported by the Romanian IFA grant CERN/ISOLDE and Nucleu project No. PN 23 21 01 02; by Spanish MCIN/AEI/10.13039/501100011033 under Grants No. RTI2018-098868-B-I00 and No. PID2021-126998OB-I00, and by Grupo de Física Nuclear (910059) at Universidad Complutense de Madrid; by German BMBF under contract 05P21PKCI1 and Verbundprojekt 05P2021; by the Generalitat Valenciana PROMETEO CIPROM/2022/9 project and by the Ministerio de Ciencia e Innovación Grant PID2022-138297NB-C21; also the Centro de Excelencia Severo Ochoa CEX2023-001292-S grant funded by MCIU/AEI is acknowledged. This work was supported by the Fonds de la Recherche Scientifique (F.R.S.-FNRS) and the Fonds Wetenschappelijk Onderzoek - Vlaanderen (FWO) under the EOS Project nr O022818F, IRI Project I002619N and IRI Project I001323N, by GOA/2015/010 and C14/22/104 (BOF KU Leuven), the Interuniversity Attraction Poles Programme initiated by the Belgian Science Policy Office (BriX network P7/12), by the ENSAR2: European Union's Horizon 2020 research and innovation programme under grant agreement No 654002, by the U.K. Science and Technology Facilities Council through Grant Nos. ST/P004598/1, ST/V001027/1, ST/Y000285/1 and ST/Y000242/1, by the Slovak Research and Development Agency (Contract No. APVV-22-0282), by the Slovak grant agency VEGA (Contract No. 1/0019/25); by the Max Planck Society, the German Federal Ministry of Education and Research (BMBF) (Grants No. 05P15HGCIA, 05P18HGCIA, and No. 05P15ODCIA) and by the French IN2P3. A. A. is grateful for financial support from the Chinese Academy of Sciences President's International Fellowship Initiative (Grant No. 2020VMA0017). Z. L. was supported by the National Natural Science Foundation of China (Grant No. 12135004).

APPENDIX A: RESULTS WITH DIFFERENT SPIN OPTIONS FOR ODD-ODD BISMUTH ISOTOPES

As indicated in Sec. III, there is some ambiguity in the spin assignment for odd-odd bismuth nuclides. Although the most probable spin assignments are well established [31, 33, 38], other spin options cannot be definitely ruled out. For completeness, in Table III the results of fitting with all possible spin assignments are presented along with the $\mu_{\rm add}$ values.

TABLE III. Spin-parity assignments (I^π), IS ($\delta\nu_{A,209}$), hfs constants (a_2, b_1), changes in mean-squared charge radius ($\delta\langle r^2\rangle_{A,209}$), magnetic ($\mu$), and quadrupole ($Q_s$) moments for investigated Bi nuclei. In the seventh column, the results of the additivity-relation calculation for odd-odd nuclides are shown ($\mu_{\rm add}$). The statistical and systematic uncertainties of $\delta\langle r^2\rangle_{A,209}$ and μ are shown in round and curly brackets, respectively. The latter values originate from the uncertainty of the F and M factors for $\delta\langle r^2\rangle_{A,209}$ and from the uncertainty of the hyperfine anomaly for μ. The results with preferable spin assignment are highlighted in bold.

A	I^π	$\delta\nu_{A,209}$ (MHz)	$\delta\langle r^2\rangle_{A,209}$(fm^2)	a_2 (MHz)	$\mu(\mu_N)$	$\mu_{\rm add}(\mu_N)$	b_1(MHz)	Q_s(b)
214g	**1$^-$**	**12750(140)**	**0.532(6){23}**	**1438(130)**	**0.265(24){3}**	**0.28**	**0**[a]	**0**
214m	(7$^-$)	12940(300)	0.540(13){23}	1737(70)	2.25(9){2}	1.98	−230(500)	−0.32(69)
	(8$^-$)	**12880(300)**	**0.538(13){23}**	**1520(70)**	**2.25(10){2}**	**2.26**	**−230(500)**	**−0.31(69)**
	(9$^-$)	12830(300)	0.536(13){23}	1372(70)	2.28(12){2}	2.54	−220(500)	−0.30(69)
216g	(7$^-$)	17580(130)	0.734(5){31}	1726(25)	2.230(32){22}	1.98	−140(100)	−0.19(14)
	(8$^-$)	**17520(130)**	**0.731(5){31}**	**1523(25)**	**2.249(37){22}**	**2.27**	**−120(100)**	**−0.17(14)**
	(9$^-$)	17540(180)	0.732(7){31}	1379(30)	2.29(5){2}	2.55	−340(200)	−0.47(28)
216m	(2$^-$)	17900(170)	0.747(7){32}	2453(50)	0.906(18){9}	0.57	190(200)	0.26(28)
	(3$^-$)	**17670(160)**	**0.738(7){31}**	**1774(40)**	**0.983(22){10}**	**0.86**	**630(200)**	**0.87(28)**
	(4$^-$)	17550(160)	0.733(7){31}	1348(40)	0.99(3){1}	1.15	760(200)	1.05(28)
218	(6$^-$)	22480(160)	0.938(7){40}	1962(18)	2.173(20){22}	1.72	800(200)	1.10(28)
	(7$^-$)	22410(160)	0.935(7){40}	1701(16)	2.199(21){22}	2.01	810(200)	1.11(28)
	(8$^-$)	**22350(160)**	**0.933(7){40}**	**1501(14)**	**2.218(21){22}**	**2.30**	**810(200)**	**1.12(28)**

[a] Fixed.

APPENDIX B: ELECTRONIC FACTORS AND UNCERTAINTIES OF $\delta\langle r^2\rangle$

The estimation of systematic uncertainties of the $\delta\langle r^2\rangle$ values is of key significance when the isotonic dependencies are studied. The main contribution to the total $\delta\langle r^2\rangle$ uncertainties stems from the uncertainty of the corresponding F factor, see Table I.

In the framework of state-of-the-art atomic calculations using a coupled-cluster method or multiconfiguration Dirac-Hartree-Fock approach, the theoretical uncertainty in the $\delta\langle r^2\rangle$ values was estimated for the bismuth (5% [32]), astatine (5% [54]), francium (3% [56]), and radium (5% [57]) atoms. For polonium, total uncertainties in $\delta\langle r^2\rangle$ values were estimated to be $\approx 5\%$ [52].

The electronic factor F for the 283-nm transition in lead is calculated usually by the King-plot procedure taking into account K X-ray, muonic atom, and elastic electron scattering data. Different versions of this procedure were used in Refs. [58] and [51]. For the lead isotopes, we adopted the F factor from Ref. [51] with an uncertainty of 9% which covers the mean difference between $\delta\langle r^2\rangle$ values obtained in Ref. [51] and Ref. [58].

Unfortunately, only the result of the semiempirical (SE) F-factor calculation is available for radon isotopes [15, 18]. It was established, however, that the SE method as a rule overestimates F factor by $10-30\%$ [14, 57, 68, 69]. In the present work, a correction factor of 15(10)% was accepted taking into account the different F-factor data for the xenon atom which has a similar electronic structure [69, 70]. It is worth noting that the same correction factor of 15% was found for adjacent radium isotopes, see relevant data in Refs. [14, 57].

[1] P. A. Butler, Proc. Roy. Soc. A **476**, 20200202 (2020).
[2] P. A. Butler and W. Nazarewicz, Rev. Mod. Phys. **68**, 349 (1996).
[3] P. Möller, R. Bengtsson, B. Carlsson, P. Olivius, T. Ichikawa, H. Sagawa, and A. Iwamoto, At. Data Nucl. Data Tables **94**, 758 (2008).
[4] P. A. Butler, J. Phys. G **43**, 073002 (2016).
[5] S. E. Agbemava, A. V. Afanasjev, and P. Ring, Phys. Rev. C **93**, 044304 (2016).
[6] L. P. Gaffney, P. A. Butler, M. Scheck, A. B. Hayes, F. Wenander, M. Albers, B. Bastin, C. Bauer, A. Blazhev, S. Bönig, N. Bree, J. Cederkäll, T. Chupp, D. Cline, T. E. Cocolios, T. Davinson, H. De Witte, J. Diriken, T. Grahn, A. Herzan, M. Huyse, D. G. Jenkins, D. T. Joss, N. Kesteloot, J. Konki, M. Kowalczyk, T. Kröll, E. Kwan, R. Lutter, K. Moschner, P. Napiorkowski, J. Pakarinen, M. Pfeiffer, D. Radeck, P. Reiter, K. Reynders, S. V. Rigby, L. M. Robledo, M. Rudigier, S. Sambi, M. Seidlitz, B. Siebeck, T. Stora, P. Thoele, P. Van Duppen, M. J. Vermeulen, M. von Schmid, D. Voulot, N. Warr, K. Wimmer, K. Wrzosek-Lipska, C. Y. Wu, and M. Zielinska, Nature **497**, 199 (2013).
[7] Y. Cao, S. E. Agbemava, A. V. Afanasjev, W. Nazarewicz, and E. Olsen, Phys. Rev. C **102**, 024311 (2020).
[8] V. Spevak, N. Auerbach, and V. V. Flambaum, Phys. Rev. C **56**, 1357 (1997).
[9] V. V. Flambaum and V. A. Dzuba, Phys. Rev. A **101**, 042504 (2020).
[10] H. Iimura and F. Buchinger, Phys. Rev. C **78**, 067301

(2008).
[11] E. Verstraelen, A. Teigelhöfer, W. Ryssens, F. Ames, A. Barzakh, M. Bender, R. Ferrer, S. Goriely, P.-H. Heenen, M. Huyse, P. Kunz, J. Lassen, V. Manea, S. Raeder, and P. Van Duppen, Phys. Rev. C **100**, 044321 (2019).
[12] I. Angeli and K. Marinova, At. Data Nucl. Data Tables **99**, 69 (2013).
[13] X. Yang, S. Wang, S. Wilkins, and R. Garcia Ruiz, Prog. Part. Nucl. Phys. **129**, 104005 (2023).
[14] S. Ahmad, W. Klempt, R. Neugart, E. Otten, P.-G. Reinhard, G. Ulm, and K. Wendt, Nucl. Phys. A **483**, 244 (1988).
[15] E. W. Otten, in *Treatise on Heavy Ion Science: Volume 8: Nuclear Far From Stability*, edited by D. A. Bromley (Springer, Boston, MA, 1989) pp. 517–638.
[16] G. Leander and R. Sheline, Nucl. Phys. A **413**, 375 (1984).
[17] A. E. Barzakh, J. G. Cubiss, A. N. Andreyev, M. D. Seliverstov, B. Andel, S. Antalic, P. Ascher, D. Atanasov, D. Beck, J. Bieroń, K. Blaum, C. Borgmann, M. Breitenfeldt, L. Capponi, T. E. Cocolios, T. Day Goodacre, X. Derkx, H. De Witte, J. Elseviers, D. V. Fedorov, V. N. Fedosseev, S. Fritzsche, L. P. Gaffney, S. George, L. Ghys, F. P. Heßberger, M. Huyse, N. Imai, Z. Kalaninová, D. Kisler, U. Köster, M. Kowalska, S. Kreim, J. F. W. Lane, V. Liberati, D. Lunney, K. M. Lynch, V. Manea, B. A. Marsh, S. Mitsuoka, P. L. Molkanov, Y. Nagame, D. Neidherr, K. Nishio, S. Ota, D. Pauwels, L. Popescu, D. Radulov, E. Rapisarda, J. P. Revill, M. Rosenbusch, R. E. Rossel, S. Rothe, K. Sandhu, L. Schweikhard, S. Sels, V. L. Truesdale, C. Van Beveren, P. Van den Bergh, P. Van Duppen, Y. Wakabayashi, K. D. A. Wendt, F. Wienholtz, B. W. Whitmore, G. L. Wilson, R. N. Wolf, and K. Zuber, Phys. Rev. C **99**, 054317 (2019).
[18] W. Borchers, R. Neugart, E. W. Otten, H. T. Duong, G. Ulm, K. Wendt, and the ISOLDE Collaboration, Hyperfine Interact. **34**, 25 (1987).
[19] I. Budinčević, J. Billowes, M. L. Bissell, T. E. Cocolios, R. P. de Groote, S. De Schepper, V. N. Fedosseev, K. T. Flanagan, S. Franchoo, R. F. Garcia Ruiz, H. Heylen, K. M. Lynch, B. A. Marsh, G. Neyens, T. J. Procter, R. E. Rossel, S. Rothe, I. Strashnov, H. H. Stroke, and K. D. A. Wendt, Phys. Rev. C **90**, 014317 (2014).
[20] K. M. Lynch, S. G. Wilkins, J. Billowes, C. L. Binnersley, M. L. Bissell, K. Chrysalidis, T. E. Cocolios, T. D. Goodacre, R. P. de Groote, G. J. Farooq-Smith, D. V. Fedorov, V. N. Fedosseev, K. T. Flanagan, S. Franchoo, R. F. Garcia Ruiz, W. Gins, R. Heinke, A. Koszorús, B. A. Marsh, P. L. Molkanov, P. Naubereit, G. Neyens, C. M. Ricketts, S. Rothe, C. Seiffert, M. D. Seliverstov, H. H. Stroke, D. Studer, A. R. Vernon, K. D. A. Wendt, and X. F. Yang, Phys. Rev. C **97**, 024309 (2018).
[21] D. A. Fink, T. E. Cocolios, A. N. Andreyev, S. Antalic, A. E. Barzakh, B. Bastin, D. V. Fedorov, V. N. Fedosseev, K. T. Flanagan, L. Ghys, A. Gottberg, M. Huyse, N. Imai, T. Kron, N. Lecesne, K. M. Lynch, B. A. Marsh, D. Pauwels, E. Rapisarda, S. D. Richter, R. E. Rossel, S. Rothe, M. D. Seliverstov, A. M. Sjödin, C. Van Beveren, P. Van Duppen, and K. D. A. Wendt, Phys. Rev. X **5**, 011018 (2015).
[22] R. Catherall, W. Andreazza, M. Breitenfeldt, A. Dorsival, G. J. Focker, T. P. Gharsa, G. T. J, J.-L. Grenard, F. Locci, P. Martins, S. Marzari, J. Schipper, A. Shornikov, and T. Stora, J. Phys. G **44**, 094002 (2017).
[23] V. Fedosseev, K. Chrysalidis, T. D. Goodacre, B. Marsh, S. Rothe, C. Seiffert, and K. Wendt, J. Phys. G **44**, 084006 (2017).
[24] S. Rothe, T. Day Goodacre, D. Fedorov, V. Fedosseev, B. Marsh, P. Molkanov, R. Rossel, M. Seliverstov, M. Veinhard, and K. Wendt, Nucl. Instrum. Methods Phys. Res., Sect. B **376**, 91 (2016).
[25] M. Seliverstov, A. Barzakh, R. Ahmed, K. Chrysalidis, T. D. Goodacre, D. Fedorov, V. Fedoseev, C. Granados, B. Marsh, P. Molkanov, V. Panteleev, R. E. Rossel, S. Rothe, S. Wilkins, and IS608 Collaboration, Hyperfine Interact. **241**, 40 (2020).
[26] S. Rothe, V. Fedosseev, T. Kron, B. Marsh, R. Rossel, and K. Wendt, Nucl. Instrum. Methods Phys. Res., Sect. B **317**, 561 (2013).
[27] M. D. Seliverstov, T. E. Cocolios, W. Dexters, A. N. Andreyev, S. Antalic, A. E. Barzakh, B. Bastin, J. Büscher, I. G. Darby, D. V. Fedorov, V. N. Fedosseev, K. T. Flanagan, S. Franchoo, G. Huber, M. Huyse, M. Keupers, U. Köster, Y. Kudryavtsev, B. A. Marsh, P. L. Molkanov, R. D. Page, A. M. Sjödin, I. Stefan, P. Van Duppen, M. Venhart, and S. G. Zemlyanoy, Phys. Rev. C **89**, 034323 (2014).
[28] R. Wolf, F. Wienholtz, D. Atanasov, D. Beck, K. Blaum, C. Borgmann, F. Herfurth, M. Kowalska, S. Kreim, Y. A. Litvinov, D. Lunney, V. Manea, D. Neidherr, M. Rosenbusch, L. Schweikhard, J. Stanja, and K. Zuber, Int. J. Mass Spectrom. **349-350**, 123 (2013).
[29] A. E. Barzakh, D. Atanasov, A. N. Andreyev, M. A. Monthery, N. A. Althubiti, B. Andel, S. Antalic, K. Blaum, T. E. Cocolios, J. G. Cubiss, P. Van Duppen, T. D. Goodacre, A. de Roubin, G. J. Farooq-Smith, D. V. Fedorov, V. N. Fedosseev, D. A. Fink, L. P. Gaffney, L. Ghys, R. D. Harding, M. Huyse, N. Imai, S. Kreim, D. Lunney, K. M. Lynch, V. Manea, B. A. Marsh, Y. M. Palenzuela, P. L. Molkanov, D. Neidherr, M. Rosenbusch, R. E. Rossel, S. Rothe, L. Schweikhard, M. D. Seliverstov, S. Sels, C. Van Beveren, E. Verstraelen, A. Welker, F. Wienholtz, R. N. Wolf, and K. Zuber, Phys. Rev. C **101**, 064321 (2020).
[30] "ISOLDE Decay Station," `https://isolde-ids.web.cern.ch/`, [Online; accessed 04.05.2025].
[31] B. Andel, P. Van Duppen, A. N. Andreyev, A. Blazhev, H. Grawe, R. Lică, H. Naïdja, M. Stryjczyk, A. Algora, S. Antalic, A. Barzakh, J. Benito, G. Benzoni, T. Berry, M. J. G. Borge, K. Chrysalidis, C. Clisu, C. Costache, J. G. Cubiss, H. De Witte, D. V. Fedorov, V. N. Fedosseev, L. M. Fraile, H. O. U. Fynbo, P. T. Greenlees, L. J. Harkness-Brennan, M. Huyse, A. Illana, J. Jolie, D. S. Judson, J. Konki, I. Lazarus, M. Madurga, N. Marginean, R. Marginean, C. Mihai, B. A. Marsh, P. Molkanov, P. Mosat, J. R. Murias, E. Nacher, A. Negret, R. D. Page, S. Pascu, A. Perea, V. Pucknell, P. Rahkila, E. Rapisarda, K. Rezynkina, V. Sánchez-Tembleque, K. Schomacker, M. D. Seliverstov, C. Sotty, L. Stan, C. Sürder, O. Tengblad, V. Vedia, S. Viñals, R. Wadsworth, and N. Warr (IDS Collaboration), Phys. Rev. C **104**, 054301 (2021).
[32] A. Barzakh, A. N. Andreyev, C. Raison, J. G. Cubiss, P. Van Duppen, S. Péru, S. Hilaire, S. Goriely, B. Andel, S. Antalic, M. Al Monthery, J. C. Berengut, J. Bieroń, M. L. Bissell, A. Borschevsky, K. Chrysalidis, T. E. Cocolios, T. Day Goodacre, J.-P. Dognon, M. Elantkowska,

E. Eliav, G. J. Farooq-Smith, D. V. Fedorov, V. N. Fedosseev, L. P. Gaffney, R. F. Garcia Ruiz, M. Godefroid, C. Granados, R. D. Harding, R. Heinke, M. Huyse, J. Karls, P. Larmonier, J. G. Li, K. M. Lynch, D. E. Maison, B. A. Marsh, P. Molkanov, P. Mosat, A. V. Oleynichenko, V. Panteleev, P. Pyykkö, M. L. Reitsma, K. Rezynkina, R. E. Rossel, S. Rothe, J. Ruczkowski, S. Schiffmann, C. Seiffert, M. D. Seliverstov, S. Sels, L. V. Skripnikov, M. Stryjczyk, D. Studer, M. Verlinde, S. Wilman, and A. V. Zaitsevskii, Phys. Rev. Lett. **127**, 192501 (2021).

[33] B. Andel, A. N. Andreyev, A. Blazhev, R. Lică, H. Naïdja, M. Stryjczyk, P. Van Duppen, A. Algora, S. Antalic, A. Barzakh, J. Benito, G. Benzoni, T. Berry, M. J. G. Borge, K. Chrysalidis, C. Clisu, C. Costache, J. G. Cubiss, H. De Witte, D. V. Fedorov, V. N. Fedosseev, L. M. Fraile, H. O. U. Fynbo, P. T. Greenlees, L. J. Harkness-Brennan, M. Huyse, A. Illana, J. Jolie, D. S. Judson, J. Konki, I. Lazarus, M. Madurga, N. Marginean, R. Marginean, B. A. Marsh, C. Mihai, P. L. Molkanov, P. Mosat, J. R. Murias, E. Nacher, A. Negret, R. D. Page, S. Pascu, A. Perea, V. Pucknell, P. Rahkila, E. Rapisarda, K. Rezynkina, V. Sánchez-Tembleque, K. Schomacker, M. D. Seliverstov, C. Sotty, L. Stan, C. Sürder, O. Tengblad, V. Vedia, S. Viñals, R. Wadsworth, and N. Warr (IDS Collaboration), Phys. Rev. C **109**, 064321 (2024).

[34] A. Andreyev, unpublished (2024).

[35] J. Kurpeta, A. Płochocki, A. Andreyev, J. Äystö, A. De Smet, H. De Witte, A.-H. Evensen, V. Fedoseyev, S. Franchoo, M. Górska, H. Grawe, M. Huhta, M. Huyse, Z. Janas, A. Jokinen, M. Karny, E. Kugler, U. Kurcewicz, W. Köster, J. Lettry, A. Nieminen, K. Partes, M. Ramdhane, H. Ravn, K. Rykaczewski, J. Szerypo, K. Van de Vel, P. Van Duppen, L. Weissman, G. Walter, A. Wöhr, and IS387 Collaboration, and The ISOLDE Collaboration, Eur. Phys. J. A **18**, 31 (2003).

[36] J. Kurpeta, A. Płochocki, A. Andreyev, J. Äystö, A. De Smet, H. De Witte, A.-H. Evensen, V. Fedoseyev, S. Franchoo, M. Górska, M. Huhta, M. Huyse, Z. Janas, A. Jokinen, M. Karny, E. Kugler, U. Kurcewicz, W. Köster, J. Lettry, A. Nieminen, K. Partes, M. Ramdhane, H. Ravn, K. Rykaczewski, J. Szerypo, K. Van de Vel, P. Van Duppen, L. Weissman, G. Walter, A. Wöhr, and IS387 Collaboration, and The ISOLDE Collaboration, Eur. Phys. J. A **18**, 5 (2003).

[37] A. Gottardo, J. J. Valiente-Dobón, G. Benzoni, S. Lunardi, A. Gadea, A. Algora, N. Al-Dahan, G. de Angelis, Y. Ayyad, D. Bazzacco, J. Benlliure, P. Boutachkov, M. Bowry, A. Bracco, A. M. Bruce, M. Bunce, F. Camera, E. Casarejos, M. L. Cortes, F. C. L. Crespi, A. Corsi, A. M. Denis Bacelar, A. Y. Deo, C. Domingo-Pardo, M. Doncel, T. Engert, K. Eppinger, G. F. Farrelly, F. Farinon, E. Farnea, H. Geissel, J. Gerl, N. Goel, M. Górska, J. Grebosz, E. Gregor, T. Habermann, R. Hoischen, R. Janik, P. R. John, S. Klupp, I. Kojouharov, N. Kurz, S. M. Lenzi, S. Leoni, S. Mandal, R. Menegazzo, D. Mengoni, B. Million, V. Modamio, A. I. Morales, D. R. Napoli, F. Naqvi, R. Nicolini, C. Nociforo, M. Pfützner, S. Pietri, Z. Podolyák, A. Prochazka, W. Prokopowicz, F. Recchia, P. H. Regan, M. W. Reed, D. Rudolph, E. Sahin, H. Schaffner, A. Sharma, B. Sitar, D. Siwal, K. Steiger, P. Strmen, T. P. D. Swan, I. Szarka, C. A. Ur, P. M. Walker, H. Weick, O. Wieland, and H.-J. Wollersheim, Phys. Rev. C **90**, 034317 (2014).

[38] H. De Witte, A. N. Andreyev, I. N. Borzov, E. Caurier, J. Cederkäll, A. D. Smet, S. Eeckhaudt, D. V. Fedorov, V. N. Fedosseev, S. Franchoo, M. Górska, H. Grawe, G. Huber, M. Huyse, Z. Janas, U. Köster, W. Kurcewicz, J. Kurpeta, A. Płochocki, K. Van de Vel, P. Van Duppen, and L. Weissman, Phys. Rev. C **69**, 044305 (2004).

[39] A. I. Morales, G. Benzoni, A. Gottardo, J. J. Valiente-Dobón, N. Blasi, A. Bracco, F. Camera, F. C. L. Crespi, A. Corsi, S. Leoni, B. Million, R. Nicolini, O. Wieland, A. Gadea, S. Lunardi, M. Górska, P. H. Regan, Z. Podolyák, M. Pfützner, S. Pietri, P. Boutachkov, H. Weick, J. Grebosz, A. M. Bruce, J. A. Núñez, A. Algora, N. Al-Dahan, Y. Ayyad, N. Alkhomashi, P. R. P. Allegro, D. Bazzacco, J. Benlliure, M. Bowry, M. Bunce, E. Casarejos, M. L. Cortes, A. M. D. Bacelar, A. Y. Deo, G. de Angelis, C. Domingo-Pardo, M. Doncel, Z. Dombradi, T. Engert, K. Eppinger, G. F. Farrelly, F. Farinon, E. Farnea, H. Geissel, J. Gerl, N. Goel, E. Gregor, T. Habermann, R. Hoischen, R. Janik, S. Klupp, I. Kojouharov, N. Kurz, S. Mandal, R. Menegazzo, D. Mengoni, D. R. Napoli, F. Naqvi, C. Nociforo, A. Prochazka, W. Prokopowicz, F. Recchia, R. V. Ribas, M. W. Reed, D. Rudolph, E. Sahin, H. Schaffner, A. Sharma, B. Sitar, D. Siwal, K. Steiger, P. Strmen, T. P. D. Swan, I. Szarka, C. A. Ur, P. M. Walker, and H.-J. Wollersheim, Phys. Rev. C **89**, 014324 (2014).

[40] J. Kurpeta, A. Andreyev, J. Äystö, A.-H. Evensen, M. Huhta, M. Huyse, A. Jokinen, M. Karny, E. Kugler, J. Lettry, A. Nieminen, A. Płochocki, M. Ramdhane, H. Ravn, K. Rykaczewski, J. Szerypo, P. Van Duppen, G. Walter, A. Wöhr, and The ISOLDE Collaboration, Eur. Phys. J. A **7**, 49 (2000).

[41] F. Kondev, M. Wang, W. Huang, S. Naimi, and G. Audi, Chin. Phys. C **45**, 030001 (2021).

[42] E. Lingeman, J. Konijn, P. Polak, and A. Wapstra, Nucl. Phys. A **133**, 630 (1969).

[43] Z. Berant, R. B. Schuhmann, D. E. Alburger, W. T. Chou, R. L. Gill, E. K. Warburton, and C. Wesselborg, Phys. Rev. C **43**, 1639 (1991).

[44] R. J. Hull and G. O. Brink, Phys. Rev. A **1**, 685 (1970).

[45] S. Schmidt, J. Billowes, M. Bissell, K. Blaum, R. Garcia Ruiz, H. Heylen, S. Malbrunot-Ettenauer, G. Neyens, W. Nörtershäuser, G. Plunien, S. Sailer, V. Shabaev, L. Skripnikov, I. Tupitsyn, A. Volotka, and X. Yang, Phys. Lett. B **779**, 324 (2018).

[46] M. Bissel, unpublished (2021).

[47] P. Campbell, I. Moore, and M. Pearson, Prog. Part. Nucl. Phys. **86**, 127 (2016).

[48] M. R. Pearson, P. Campbell, K. Leerungnavarat, J. Billowes, I. S. Grant, M. Keim, J. Kilgallon, I. D. Moore, R. Neugart, M. Neuroth, S. Wilbert, and the ISOLDE Collaboration, J. Phys. G **26**, 1829 (2000).

[49] A. E. Barzakh, D. V. Fedorov, V. S. Ivanov, P. L. Molkanov, F. V. Moroz, S. Y. Orlov, V. N. Panteleev, M. D. Seliverstov, and Y. M. Volkov, Phys. Rev. C **95**, 044324 (2017).

[50] W. J. Tomlinson and H. H. Stroke, Phys. Rev. Lett. **8**, 436 (1962).

[51] M. Anselment, W. Faubel, S. Göring, A. Hanser, G. Meisel, H. Rebel, and G. Schatz, Nucl. Phys. A **451**, 471 (1986).

[52] T. E. Cocolios, W. Dexters, M. D. Seliverstov, A. N. Andreyev, S. Antalic, A. E. Barzakh, B. Bastin, J. Büscher, I. G. Darby, D. V. Fedorov, V. N. Fedosseyev, K. T. Flanagan, S. Franchoo, S. Fritzsche, G. Huber, M. Huyse, M. Keupers, U. Köster, Y. Kudryavtsev, E. Mané, B. A. Marsh, P. L. Molkanov, R. D. Page, A. M. Sjoedin, I. Stefan, J. Van de Walle, P. Van Duppen, M. Venhart, S. G. Zemlyanoy, M. Bender, and P.-H. Heenen, Phys. Rev. Lett. **106**, 052503 (2011).

[53] B. Cheal, T. E. Cocolios, and S. Fritzsche, Phys. Rev. A **86**, 042501 (2012).

[54] J. G. Cubiss, A. E. Barzakh, M. D. Seliverstov, A. N. Andreyev, B. Andel, S. Antalic, P. Ascher, D. Atanasov, D. Beck, J. Bieroń, K. Blaum, C. Borgmann, M. Breitenfeldt, L. Capponi, T. E. Cocolios, T. Day Goodacre, X. Derkx, H. De Witte, J. Elseviers, D. V. Fedorov, V. N. Fedosseev, S. Fritzsche, L. P. Gaffney, S. George, L. Ghys, F. P. Heßberger, M. Huyse, N. Imai, Z. Kalaninová, D. Kisler, U. Köster, M. Kowalska, S. Kreim, J. F. W. Lane, V. Liberati, D. Lunney, K. M. Lynch, V. Manea, B. A. Marsh, S. Mitsuoka, P. L. Molkanov, Y. Nagame, D. Neidherr, K. Nishio, S. Ota, D. Pauwels, L. Popescu, D. Radulov, E. Rapisarda, J. P. Revill, M. Rosenbusch, R. E. Rossel, S. Rothe, K. Sandhu, L. Schweikhard, S. Sels, V. L. Truesdale, C. Van Beveren, P. Van den Bergh, Y. Wakabayashi, P. Van Duppen, K. D. A. Wendt, F. Wienholtz, B. W. Whitmore, G. L. Wilson, R. N. Wolf, and K. Zuber, Phys. Rev. C **97**, 054327 (2018).

[55] V. A. Dzuba, W. R. Johnson, and M. S. Safronova, Phys. Rev. A **72**, 022503 (2005).

[56] M. R. Kalita, J. A. Behr, A. Gorelov, M. R. Pearson, A. C. DeHart, G. Gwinner, M. J. Kossin, L. A. Orozco, S. Aubin, E. Gomez, M. S. Safronova, V. A. Dzuba, and V. V. Flambaum, Phys. Rev. A **97**, 042507 (2018).

[57] L. W. Wansbeek, S. Schlesser, B. K. Sahoo, A. E. L. Dieperink, C. J. G. Onderwater, and R. G. E. Timmermans, Phys. Rev. C **86**, 015503 (2012).

[58] G. Fricke and K. Heilig, in *Nuclear Charge Radii*, edited by H. Schopper (Springer, Berlin, Heidelberg, 2004) pp. 1–385.

[59] I. Angeli, Y. P. Gangrsky, K. P. Marinova, I. N. Boboshin, S. Y. Komarov, B. S. Ishkhanov, and V. V. Varlamov, J. Phys. G **36**, 085102 (2009).

[60] A. E. Barzakh and V. P. Denisov, Z. Phys. A **346**, 265 (1993).

[61] B. A. Brown and K. Minamisono, Phys. Rev. C **106**, L011304 (2022).

[62] S. A. Ahmad, W. Klempt, C. Ekström, R. Neugart, and K. Wendt, Z. Phys. A **321**, 35 (1985).

[63] P. Möller, J. Nix, W. Myers, and W. Swiatecki, At. Data Nucl. Data Tables **59**, 185 (1995).

[64] G. A. Leander and Y. S. Chen, Phys. Rev. C **37**, 2744 (1988).

[65] G. Neyens, Rep. Prog. Phys. **66**, 633 (2003).

[66] L. V. Skripnikov and A. E. Barzakh, Phys. Rev. C **109**, 024315 (2024).

[67] A. E. Barzakh, D. V. Fedorov, V. S. Ivanov, P. L. Molkanov, F. V. Moroz, S. Y. Orlov, V. N. Panteleev, M. D. Seliverstov, and Y. M. Volkov, Phys. Rev. C **97**, 014322 (2018).

[68] G. Torbohm, B. Fricke, and A. Rosén, Phys. Rev. A **31**, 2038 (1985).

[69] J. Libert, B. Roussière, and J. Sauvage, Nucl. Phys. A **786**, 47 (2007).

[70] R. Silwal, A. Lapierre, J. D. Gillaspy, J. M. Dreiling, S. A. Blundell, Dipti, A. Borovik, G. Gwinner, A. C. C. Villari, Y. Ralchenko, and E. Takacs, Phys. Rev. A **98**, 052502 (2018).